Eur Biophys J (1997) 25: 225–237

ARTICLE

Cyril Favard · Jeanne Pager · Daniel Locker
Paul Vigny

Incorporation of ethidium bromide in the *Drosophila* salivary gland approached by microspectrofluorometry: evidence for the presence of both free and bound dye in the nuclei of cells in viable conditions

Received: 23 November 1995 / Accepted: 9 September 1996

Abstract The incorporation of 10^{-6} M ethidium bromide (EB) was studied in viable *Drosophila melanogaster* salivary glands with a spatial resolution reaching a few μm^3, using a confocal laser microspectrofluorometer designed for spectral analysis. Spectra were recorded with the 514 nm Argon laser line during excitation times of 1 second (20 μW on the preparation) at 5 min intervals for 30 or 60 min, either at points in determined cell sites or serially throughout the cells. The fluorescence intensity time-course indicated that the EB intake was not an all-or-none process, but rather a graded, sensitive indicator of the functional state of the cell. On the micrometer scale, the cytoplasm behaved as an homogeneous substrate with the fluorescence intensity depending on EB intake and intracellular diffusion. In the nucleus, however, localized enhancement of the emission intensity was observed. Spectral analysis allowed us to characterize the interactions. The mean values of λ_{max} in the cytoplasm (600 nm), in the nucleus (601 nm) and outside the glands (602 nm) were less than for free EB in aqueous solution (630 nm); values of full width at half maximum were between 92 and 96 nm, which is much lower than the 120 nm observed for free EB. The recorded spectra were analyzed using a linear combination of two spectral models, namely free and DNA intercalated EB. In the nucleus, the free EB model spectra was found to represent up to 10% of the recorded spectra whereas it was near zero in the cytoplasm. The present data suggest that the intranuclear concentration of free EB (allowing for its lower fluorescence quantum yield) might be at least equal to that of the bound EB.

Key words Fluorescence spectroscopy · Spectral imaging · Ethidium bromide · In vivo · Salivary glands

C. Favard · J. Pager · D. Locker · P. Vigny (✉)
Centre de Biophysique Moléculaire,
CNRS, UPR 4301 conventionnée avec l'Université d'Orléans,
Rue Charles-Sadron, F-45071 Orléans Cedex 2, France

Abbreviations bp base pair · CCD charge coupled device · CY cytoplasm · DNA deoxyribonucleic acid · RNA ribonucleic acid · EB ethidium bromide · EX external medium · FI fluorescence intensity · FWHM full width at half-maximum · HN high nuclear fluorescence · LN low nuclear fluorescence · MB plasma membrane · NU nucleus · nu nucleolus · PBS phosphate buffered saline

Introduction

Knowledge about genetic expression derives mainly from data obtained either in vitro, or in cells fixed and treated for histology. It is clear however that models accounting for chromatin functions ought to be checked in vivo, at appropriate spatial resolution, and this involves the selection of accurate methodologies. Spectral fluorescence analysis can bring out information on the nature, properties, chemical environment and relative proximity of molecules taking part in life processes. Recently, microspectrofluorometers have been designed with the prospect of biological studies. The prototype now at our disposal (V45 built by DILOR, Lille, France) has been described in a brief note (Valisa et al. 1995) and the general features are indicated in the Methods. It is thoroughly described in a paper by Favard et al. now in preparation. Starting from point fluorescence spectra, it can provide confocal fluorescent spectral images of living preparations, at an adjustable microscopic scale, with a suitable detection sensitivity.

As a biological model, the isolated salivary glands of *Drosophila* survive the operating conditions required for spectroscopic recording on such an apparatus. In the polytene chromosomes, the puffing phenomenon offers a classical model of gene expression, with the advantage that the band size is at least equal to the minimal volume analyzed by the microspectrofluorometer. Their intimate organization is on the way to being elucidated (Rykowski et al. 1988; Ericsson et al. 1990; Levi-setti et al. 1994; Saitoh and Laemmli 1994; Summer 1994) and their genetic function subserved classical works on gene transduction (Ash-

burner 1972, 1990; Huet et al. 1993; Woodward et al. 1994). Fluorescence investigations in vivo may be able to contribute significant information to molecular biology, noting that the salivary gland itself, as a model for biophysics in vivo, is even more complex than isolated cells. In the present state of methodology, the control of physiological parameters can hardly reach the same accuracy as that of physical parameters, which can be expected to limit the quantitative analysis of some data.

Among the nuclear fluorescent probes, some exhibit a spectrum overlapping cellular autofluorescence; others may resemble cellular substrates, and may therefore interfere with the living cell function. Ethidium Bromide (EB) has been extensively studied; it is interesting for our purpose related to the staining of chromatin. The modes of fluorescent interaction between EB and nucleic acids in solution have been reviewed (Le Pecq 1972; Latt and Langlois 1990). The fluorescent dye can intercalate between base pairs of double-stranded nucleic acids, without base specificity, with a twentyfold increase in quantum yield due to hydrophobicity of the available space, as is the case for insertion of EB into hydrophobic micelles and plasma membranes (Gitler et al. 1969). Under controlled ionic strength and concentration conditions, EB may also interact electrostatically with the phosphate backbone of nucleic acids, and with proteins (Thresher and Griffith 1990) or inorganic macromolecules (Le Pecq 1972); the quantum yield is then close to that of free EB in aqueous solution. Clearly, the interaction of EB with the living cell constituents has to be examined as to the specificity towards nucleic acids.

Ethidium bromide can be used as a structural probe, since the fluorescence intensity measured in fixed lymphocytes is positively correlated to the degree of chromatin dispersion in the nucleus (Santisteban et al. 1992). In vitro studies on native chromatin and isolated nuclei involving most often fluorescence, and sometimes circular dichroism, have corroborated the potential of EB as a useful probe for the structure and organization of genomic DNA. Ethidium bromide was the acceptor in an energy transfer study showing that the fluorochrome accessibility to DNA depends on the conformation and on the protein coverage (Brodie et al. 1975). Deproteinization increases the number of binding sites (Angerer and Moudrianakis 1972; Darzynkiewicz et al. 1984), and may take part in the physiological opening of condensed chromosomal interbands on puffing; as a corollary, native chromatin binds less EB than naked DNA (Paoletti et al. 1977). The chromatin of isolated nuclei binds EB in the same manner as does circular DNA (Cook and Brazell 1978), and the degree of EB intercalation was used as a measure of the proportion of puffing DNA in the nuclei and polytene chromosomes of *Drosophila* salivary glands (Gruzdev and Shurdov 1992). Native chromatin presents the same supercoiling degree as nucleosomes, and a lower affinity for EB than does linear DNA (Vergani et al. 1994). It was pointed out that the general organization of native chromosomes, where genetic units are attached as loops to the proteic axis, introduces such a mechanical stress that the punctually intercalated EB could unwind a whole loop (Paoletti 1979) and create areas of local high condensation compensating for unwinding, as observed ultrastructurally in well preserved isolated nuclei (Santi et al. 1987). Ethidium bromide, however, is not a neutral probe, and can itself deproteinize and unwind extracted chromatin; the drug/DNA ratio is a critical factor (Benyajati and Worcel 1976).

Ethidium bromide is still classically used to sort dead cells, which have lost the plasma membrane selective permeability and the chromatin organization: the nuclei are then quickly endowed with a bright orange fluorescence (Dey and Majumder 1988; Prokuryakov et al. 1989; Tekle et al. 1991; Weston et al. 1994; "Dutch" Boltz et al. 1994; Bicknell and Cohen 1995). Initially, however, EB was used in a more graded way as a viable pharmacodynamic agent, with special attention to the conditions of drug treatment. External concentrations greater than 10^{-5} M, and long exposures (sometimes, several days) could elicit significant and irreversible changes in chromatin organization (Heinen et al. 1974; Hartwig 1979; Mattern and Painter 1979) as well as impairment of chromatin condensation, thus possibly decreasing the mitotic index (Kuwano and Kajii 1991; Kattstrom and Nilsson 1992; Sumner 1992). We have therefore limited our study to the minimal levels mentioned by previous authors, i.e. 10^{-6} M in the external medium. With this order of magnitude, and with an exposure time limited to one hour, no significant mutagenic or toxic effect could be detected either in unicellular organisms or in cultured cells (Mattern and Painter 1979; Slonimski et al. 1968; Himpens et al. 1992); EB may be thus regarded as a vital stain.

The present work has been undertaken with a view to future spectral analysis of chromatin function on the scale of the genomic units, using fluorescent probes. The *Drosophila* salivary gland is a proper model for such a purpose and also for studying the uptake of permeating tracers, since the glandular cells can be approximated to prismatic volumes of about 100 μm high, into which the external substances may permeate from the base. The experiment has been designed to check the adaptability of such a biological model to the operating conditions of the microspectrofluorometer, assuming that 10^{-6} M EB was a permeant vital stain, expected to behave as an intranuclear probe of puffing chromosome regions.

In spite of some limits to quantitative studies inherent in the present experimental conditions, the spectroscopic tracing of EB uptake by the gland cells has validated the experimental approach in that the fluorescent dye could be identified in the nuclei of viable preparations, allowing spectral information to be obtained at a spatial resolution of a few μm^3. The spectral analysis of the EB uptake kinetics has given an insight to graded processes involving membrane function. More interestingly, although in the cytoplasm, EB appears to be totally involved in molecular interactions, it has shown that EB is partly free in the nucleus, which questions whether it can be reasonably regarded as a specific probe for nucleic acids.

Methods

1. Biological material

Wild *Drosophila melanogaster* (Oregon-R type) were reared on standard diet (agar-corn-yeast) at 24 °C in 70% humidity. Vivid IIIrd instar larvae, all belonging to the same 24 h span, were chosen for the experiment. The salivary glands were dissected extemporaneously, rinsed and maintained in a sterilized phosphate-buffered saline without Ca^{2+} or Mg^{2+} at pH 7 (PBS). The whole experiment was carried out at room temperature.

2. Staining solutions

The EB stock solution (Molecular Probes) was diluted to 10^{-2} M in distilled water and kept at 4 °C in the dark. Further dilutions were performed in PBS as required. The stability of the solutions was checked at the end of the experiment by measuring the absorbance at 481 nm. Moreover, the stability of the EB fluorescence emission spectrum was checked in a blank experiment in buffer.

The orcein staining solution was composed of 2% Gurr's orcein (a natural mixture of 14 staining components derived from orcinol), dissolved in glacial acetic acid and 85% lactic acid (v/v). The stain was prepared without heating, and was centrifuged for 1 min at 10^4 rpm before use.

3. Microspectrofluorometer

The experiments were carried out with a V45 microspectrofluorometer (DILOR, France), the schematic diagram of which is shown in Fig. 1. In this device, an argon ion laser (Spectra Physics, model 2065s) is used as a visible source of excitation. It passes through an adjustable beam expander to correctly focus the laser and to entirely cover the entrance aperture of the objective. The laser is then reflected by a beam-splitter and two mirrors to reach the sample. The sample is set under a conventional confocal microscope (Nikon Optiphot-2) equipped with a TV color camera for transmitted light to digitize the image. Fluorescence is collected by the objective and reaches a square shaped adjustable pinhole by the reverse pathway. The excitation line is suppressed using a holographic filter (Notch filter). The fluorescent beam is then focused on the entrance slit of the spectrograph using an achromatic lens and a mirror. The spectrograph has been stigmatically designed by the use of lenses and low focal length spherical mirror. It is equipped with a 300 grooves/mm holographic grating coupled to a bidimensional detector (CCD). The grating is driven by a sine bar (linear in wavelength), commanded by software with one nanometer precision and reproducibility. Using an ethernet card, data coming from the CCD are collected and different components of the apparatus can be driven. The PC is linked to a workstation (SUN, Sparcclassic) containing the data treatment software.

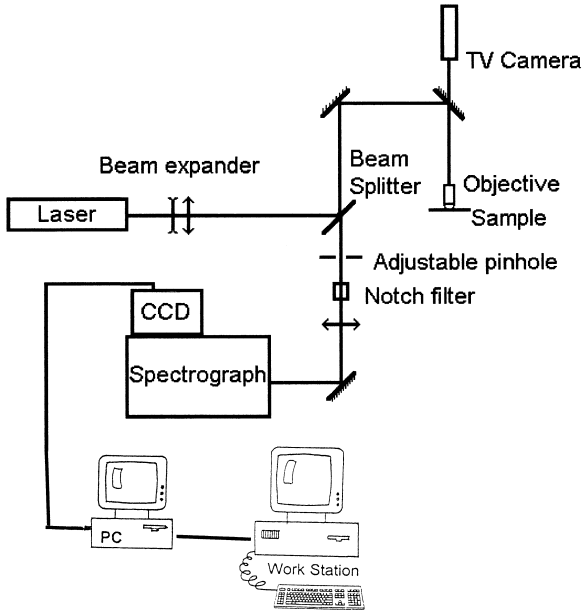

Fig. 1 Schematic diagram of the microspectrofluorometer V45 used in this study

All the measurements were made using the 514 nm line of the laser as the excitation wavelength. The laser power reaching the sample was estimated to be at most 20 μW and it was standardized by reference to the emission intensity of a uranyl bar. The spectral resolution was set to 1 μm and checked by means of a low-pressure mercury lamp.

A 40× fluorite oil immersion objective, NA = 1.3 (Nikon, France) was used. The lateral resolution was estimated to be 1 μm. In order to obtain a good signal to noise ratio, the adjustable pinhole was set to 200 μm to give a vertical depth of focus estimated as 6 μm, which is still relatively small compared to the cell dimensions.

4. Recording schedules

The freshly dissected glands were placed individually in the microchamber of a hollow glass slide in 5 μl of PBS, under a coverslip partly sealed with silicon grease. Before starting the recording of EB uptake kinetics, each gland was placed under the microscope (40×) for cell observation on the camera screen and for imaging. The cells all belonging to the secretory epithelium were chosen on the lateral edge of the gland, generally in the middle part of a lobe, with the basal membrane seen together with the external medium (Fig. 2a). The plasma and nucleus membranes, the nucleolus and the banded chromosomes could be distinguished in viable preparations. Several glands had to be discarded because the initial image definition was progressively blurred by accumulating secretion products.

Control spectra were then recorded from the following standard points, as shown in Fig. 2a: in the external medium near the gland (EX), and from one cell per gland, at

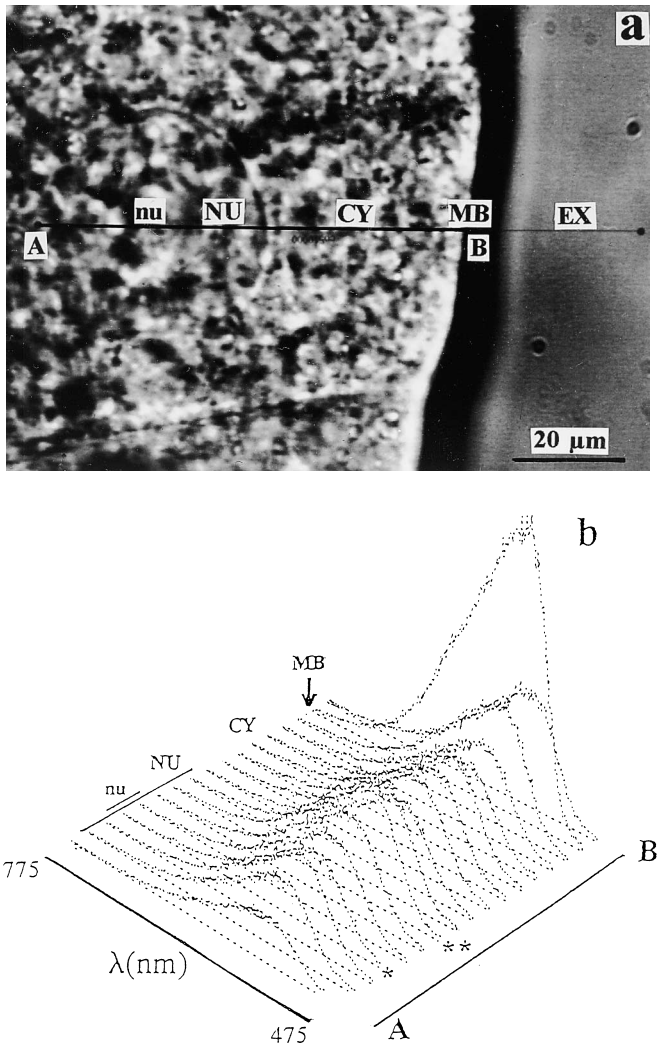

Fig. 2 **a** Directly transmitted view of a typical glandular cell. The EB uptake kinetics described in this study have been obtained by recording fluorescence spectra in the external medium (*EX*), plasma membrane (*MB*), cytoplasm (*CY*), nucleus (*NU*) and nucleolus (*nu*). Line imaging (see **b**) has been performed from *A* to *B* with 5 µm steps. AB = 80 µm. **b** Spectral line imaging along AB (5 µm steps) between 475 and 775 nm. Records from the cell displayed in (**a**), 30 min after EB addition (10^{-6} M). Single and double asterisks: depression and peak in the fluorescence intensity, corresponding respectively to a nucleolar and a chromosomal region

the external cell membrane (MB), in the cytoplasm (CY) and in the nucleus (NU). The initial recording points were chosen on the camera screen, and their coordinates were stored for automatic reset. Cell images were accessible throughout the experiment, to monitor the general state and stability of the glands. Slight movements of the preparation from the initial position were easily counterbalanced manually. The data from glands moving by several micrometers were discarded. In fact, a compromise had to be found between immobilizing the substrate and allowing free access of the external medium to the cells. The staining solution (EB, 45 µl at 1.125×10^{-6} M) was introduced under the coverslip at the starting time. The spectra were recorded serially every five minutes, for half an hour or one hour, at the same points and in the same order as for the controls. The spectra collected from the four sites (EX, MB, CY, NU) at the six successive times (5 to 30 min) were analyzed in terms of fluorescence intensity. The measurements at 5 min had a poor signal/noise ratio; for this reason, the spectral study was carried out on records at 10 and 30 min, in six preparations maintained for one hour sessions before being fixed for histological examination.

In a complement to the main kinetic experiment, several glands were submitted to one of the following treatments: osmotic shock (20 min in distilled water) and staining in PBS-EB or water-EB, or direct staining in PBS-EB 10^{-6} M. The recording schedule was either identical to the one described previously, or it consisted of linear imaging (Fig. 2b). In this case, series of spectra were recorded every 5 or 2 µm, at defined times of EB exposure, straight through the nucleus, cytoplasm, plasma membrane and the proximal external medium, along an 80 µm segment.

5. Signal processing

Before adding EB, fluorescence spectra were recorded in each chosen site in order to measure the fluorescence contribution of the cells. These blank spectra were substracted from the corresponding spectra obtained in the presence of EB. The difference spectra were then submitted to two distinct mathematical treatments. Firstly, artefactual spikes (from cosmic rays reaching the CCD) were eliminated. The spectra were then smoothed by high-frequency filtering of the direct Fourier transform and applying the inverse Fourier transform to recover the signal. The cutting frequency was fixed for all the treated spectra, introducing little or no error on the determination of the maximum of emission and the full width at half maximum.

The spectra did not have to be corrected for the apparatus response, since the overall transmission response of the apparatus is constant in the 550–650 nm region (Favard et al., in preparation).

In each site and at each time the intensity of fluorescence given in the Results is expressed in counts corresponding to the integral:

$$I = \int_{\lambda_1}^{\lambda_2} I(\lambda)\, d\lambda$$

between 550 and 700 nm, and further divided by 10^3.

In an attempt to determine the contribution of free EB (f) and bound EB (b) to each recorded spectrum, the intensity of the recorded spectrum was considered as a linear combination of the intensity of the components described above over the wavelength range:

$$\sum_{\lambda_1}^{\lambda_2} I(\lambda) = \alpha \sum_{\lambda_1}^{\lambda_2} I_b(\lambda) + \beta \sum_{\lambda_1}^{\lambda_2} I_f(\lambda)$$

The determination of the two coefficients α and β was made using a least-squares model. The percentage of error given

as a test for a good fit corresponds to:

$$E = 100.\left(\sum_{\lambda_1}^{\lambda_2} (I_{measured} - I_{calculated})^2 / \sum_{\lambda_1}^{\lambda_2} I_{calculated}^2 \right)^{1/2}$$

$$\text{with : } I_{calculated} = \alpha \sum_{\lambda_1}^{\lambda_2} I_b(\lambda) + \beta \sum_{\lambda_1}^{\lambda_2} I_f(\lambda).$$

Results

1. Line spectral imaging

Ethidium bromide at 10^{-6} M is able to enter the cells of freshly dissected, anatomically normal glands. It can be identified spectrally at 5 min in the cytoplasm, and later on in most nuclei, giving rise to characteristic ethidium fluorescence. Spectra were recorded serially in nine cells, from the external medium throughout the membrane, cytoplasm and nucleus, after 10, 20 and 30 min in the EB solution. Under the various experimental conditions mentioned in the Methods, several common features came out of the sprectral series examination as observed in Fig. 2b. The plasma membrane region appears as the most intense source of fluorescence, and the signal appears to decrease regularly (as in a diffusion model) towards the inside of the cell. With either 5 or 2 μm steps, and with a lateral resolution in the range of a micrometer, the cytoplasmic compartment does not display any noticeable fluorescence irregularity. In the nucleolar area, the fluorescence is not brighter than elsewhere in the cell, and can even be less than the level measured in the peripheral part of the nucleus, where chromosomes are generally found. In five sites localized within the same nucleus, the values of fluorescence intensity were significantly correlated to the distance from the cell membrane, i.e. to the source of ethidium ($r_s = 0.95$; $p \leq 0.05$). In contrast to the cytoplasm, the nuclear compartment presents slight spatial irregularities in the fluorescence intensity, and this was even clearer at the 2 μm resolution. From previous observations (Pager et al. 1995), this might suggest a correlation with chromosome banding. In one gland submitted to a thermal shock (30 min at 50 °C) before the EB staining, the nucleus was more brightly fluorescent than the surrounding cytoplasm (when observed in epifluorescence microscopy). In most cells submitted to an experimental osmotic shock, fluorescence was hardly detectable or not detectable at all in the nuclei, which were however easily stained in Trypan blue at the end of the experiment, indicating that the cells were dead. In the membrane records, the fluorescence intensity was reaching levels similar to those of non-shocked cells. Thus, EB cannot be regarded as an absolute probe for dead material, but can be an appropriate vital stain under given conditions.

2. Fluorescence intensity

The gland epithelial cells represent a good model to study the intracellular diffusion of permeating external substances, in that they can be approximated as prisms of cytoplasm enclosing the nearly spherical and central nucleus; substances are penetrating from the base, owing to the polarity of the secretory cells. The time-course of fluorescence intensity was examined in fourteen cells, each from one gland. The position of the recording site could be memorized in twelve of them. The cells were seen as sagittal sections of the cytoplasmic prism. In the kinetic study, the basal sections has been explored. A schematic representation of the cellular field commonly observed is displayed in Fig. 3. Ethidium bromide was penetrating leftwards, from the external medium (EX) through the basal plasma membrane (MB) into the cytoplasm (CY, hatched) and the nucleus (NU). The coordinates of the recording sites have been standardized and positioned on the same scheme. In each site and at each time, the intensity of the fluorescence emission has been expressed in arbitrary counts representing the area under the corresponding spectrum. Point measurements were performed in the four compartments, at 5 min intervals, from 5 to 30 min after the EB addition. In

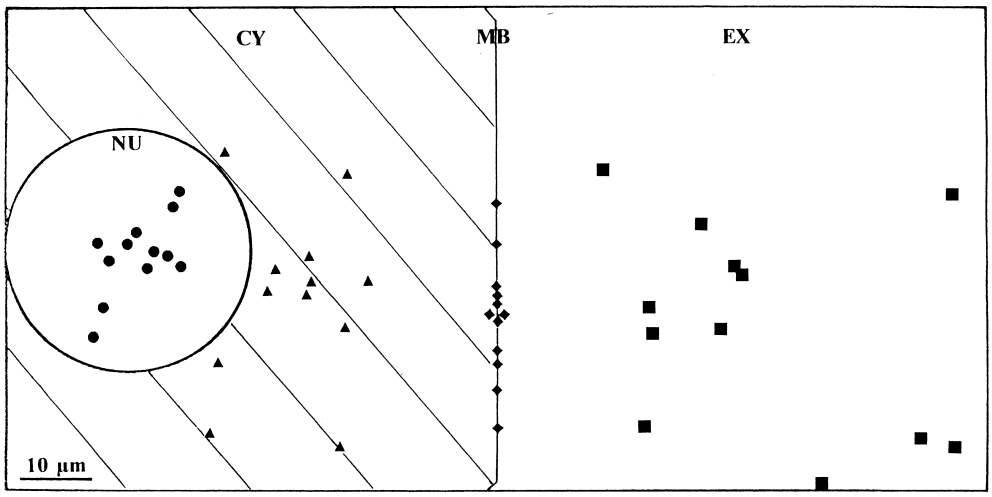

Fig. 3 Cellular localization of the recording sites. The sites have been pooled on the schematic representation of a cell sagittal view. CY: cytoplasm (hatched; ▲); MB: basal plasma membrane (◆); EX: external medium (■); NU: nucleus (●). The coordinates of the sites in the cellular sagittal plane have been standardized relative to the plasma membrane and to the center of the nucleus

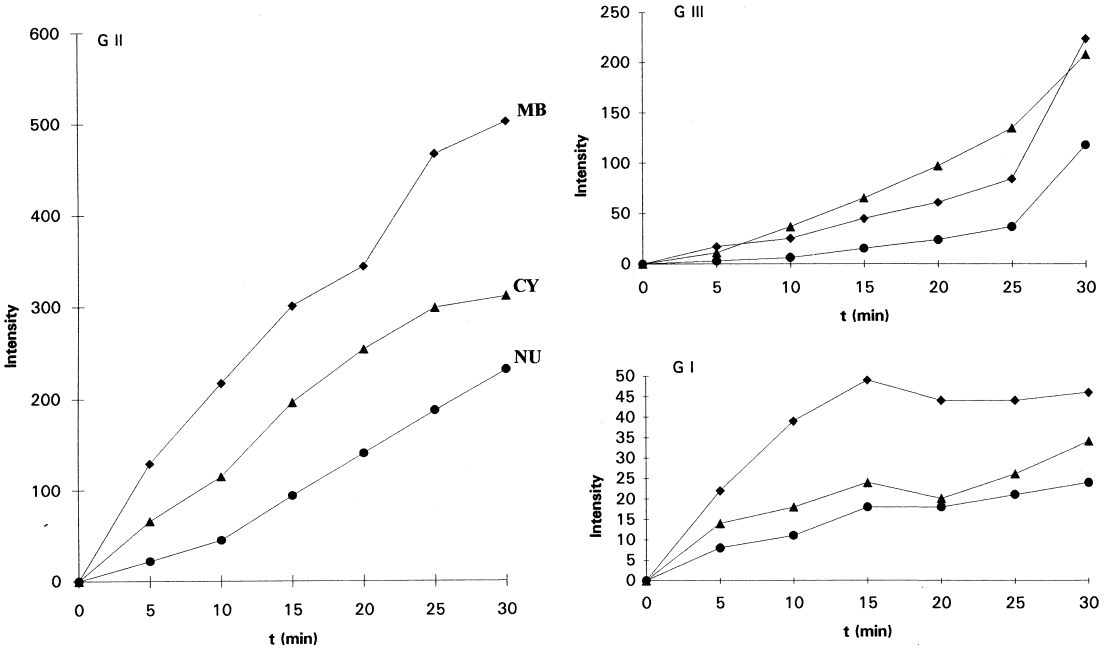

Fig. 4 Time-course of fluorescence intensity in the three groups of LN (low nuclear fluorescence) cells. Ordinate: fluorescence intensity (the integrate of counts from the fluorescence spectra, divided by 10^3). ◆: membrane (MB); ▲: cytoplasm (CY); ●: nucleus (NU)

all the cells, the fluorescence intensity was still increasing at 30 min, at least in the nucleus, and most often in all the sites.

When considering the whole set of kinetics, two families of cells could be found, according to the intracellular distribution of fluorescence intensity after 30 min of exposure to EB: either membrane > cytoplasm > nucleus, which defines LN cells (low nuclear emission, 9 items) or nucleus > membrane > cytoplasm, in the HN cells (high nuclear emission, 5 items). Another way to sort the cells was achieved by reducing each plot to two parameters: the total fluorescence intensity at 5 min (i.e. the sum of the intensities collected from the three cellular sites at this time), and the rate of fluorescence increase (i.e. the ratio of the total fluorescence intensity at 30 min to that at 5 min). When plotting the cells in the plane defined by these parameters, an L-shaped scatter was obtained (data not shown) where three groups could be defined, taking the mean values of the parameters as landmarks. The corresponding kinetics are displayed in Fig. 4, where it can be seen that the fluorescent emission could be either initially low and slowly increasing (Group I) or accelerating (Group III), or initially high and slowly developed (Group II). Three LN cells were found in each group. Inside each group, the time-courses of the fluorescence intensity in the various cell domains showed profiles significantly correlated to each other, using the concordance coefficient of Kendall (GI:$W = 0.834$; GII and GIII: $W = 1$, $p < 0.01$). Considering the total fluorescence intensities at each recording time, the three groups were found to differ significantly from each other, following the Kruskal-Wallis rank analysis of variance ($\chi^2_1 = 21.561$; $p < 0.001$).

3. Histological controls

The benign effect of laser irradiation on the cells under the present experimental conditions has been established previously (Pager et al. 1995). The glands were shown to be translucid and anatomically normal after the experiment. Four preparations have been fixed and squashed in orcein at the end of the experiment; they all presented well preserved chromosomes (data not shown). Trypan blue (0.2%, 10 min) has also been used occasionally at the end of the experiment and was excluded by the epithelial glandular cells. These criteria are commonly used in cell biology to check the viability of cells.

4. Fluorescence emission: spectral characteristics

A detailed analysis has been carried on six cells. The spectra such as those reported in Fig. 5a were recorded in the three locations defined previously. Two parameters were measured, the wavelength of the maximum of fluorescence (λ_{max}) and the full width at half maximum (fwhm). Considering that the values obtained in each cell at all the times (from 5 to 60 min each 5 min after EB addition) did not display any systematic change as a function of time, they have been pooled together and the means are regarded as being representative in each site for each cell. The λ_{max} and fwhm means are given in Table 1. In all the experiments the maximum emission wavelength within the cytoplasm was lower than those of the external medium and the nucleus in all cases. Regarding the fwhm, the values

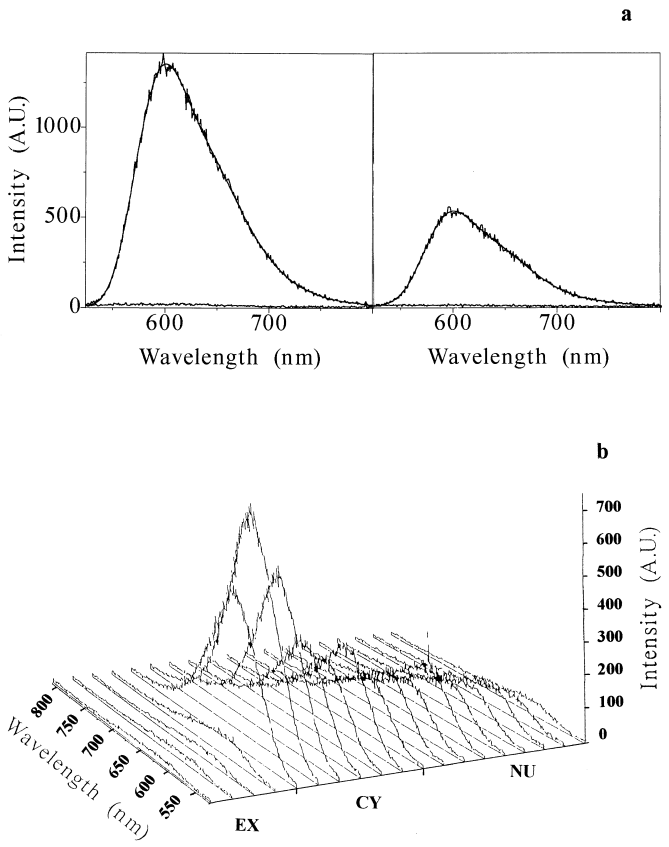

Fig. 5 **a** Typical spectra recorded from the same cell, either in the cytoplasm (*left*) or in the nucleus (*right*), 10 min after addition of EB. The superimposed spectra correspond to the raw (noisy) signal and to the signal after Fourier transform smoothing; the nearly flat traces under the spectra correspond to the cell autofluorescence. *Abscissa:* wavelength (nm; ordinate: fluorescence intensity. Recording duration: 1 s for each spectrum. Power intensity on the preparation: 20 μW. **b** Spectral line imaging across one cell exhibiting larger variation in the maximum emission wavelength when going from external medium (*EX, left side*) to the nuleus (*NU, right side*), 30 min after addition of 10^{-6} M EB in the external medium. Recording duration: 1 s for each spectrum (30 s for the set). Power intensity on the preparation: 20 μW. Spectra are recorded each 5 μm, representing 95 μm from left to right

follow the same trend and were found to be higher in the external medium than in the cytoplasm or nucleus.

Larger differences have been observed in a few cells such as that reported in Fig. 5b. This figure represents the line imaging containing 19 points recorded each 5 μm in the x direction. In such a case the λ_{max} mean values were found to be respectively 614, 599 and 600 nm in the external medium, the cytoplasm and the nucleus. This is emphasized by fwhm mean values varying from 106 nm in the external medium to 89 nm in the cytoplasm and 94 nm in the nucleus. More important is the fact that when travelling from far external medium to cellular limits, the λ_{max} and fwhm values continuously decreased from 630 nm and 120 nm to 599 nm and 90 nm in the first point of the cytoplasm. This points out the limit of calculating λ_{max} and fwhm mean values in the external medium, considering dispersion of the recording sites (see Fig. 3).

Table 1 Spectroscopic characteristics of the ethidium bromide (EB) fluorescence emission collected from various areas within the gland. EX: externally to the glands but close to the cell; CY: cytoplasm; NU: cell nucleus; FEB: free ethidium bromide in aqueous solution

Source of fluorescence	λ_{max} (nm)	fwhm (nm)
EX	602 ± 1	96 ± 5
CY	600 ± 1	92 ± 2
NU	601 ± 1	92 ± 2
FEB	630 ± 2	122 ± 5

5. Spectral decomposition

The systematic shift of the maximum emission wavelength within the cellular compartments – although small – as well as the increase of full-width at half maximum might result from the addition of several types of spectra with various weight depending on the location within the cell. In order to check this hypothesis, all the recorded spectra in the cells were firstly treated as described above and then submitted to a linear combination decomposition using the simplest two component model, ethidium bromide in water (free EB; $\lambda_{max} = 630 \pm 2$ nm, fwhm = 122 ± 5 nm) and ethidium bromide complexed to linear pBR 322 at a ratio 1:400 dye:base pair in the conditions where all the ethidium is supposed to be intercalated (bound EB; $\lambda_{max} = 600 \pm 1$ nm, fwhm = 90 ± 2 nm). The two model spectra are represented in Fig. 6 (upper part). As an example, the same figure (lower part) shows a decomposition made on a spectrum recorded in the nucleus. Free EB represents in this case 10% of the total intensity of the spectrum. The difference between the fitted and the experimental spectra plotted in the upper right corner of the figure shows the quality of the fit.

This mathematical treatment has been made on all the spectra recorded in the cells at each site and each time, i.e. on a set of 49 different experimental spectra. The mean percentage of free and bound EB in each site as well as errors obtained on the fit when using the two components or only the bound EB as a model are given in Table 2. Examination of the table surprisingly shows that nearly 10% of the total fluorescence intensity coming from the nucleus can be ascribed to free EB. The fact that the percentage of error using the two components model is lower than when using the DNA bound EB model alone confirms this hypothesis. The situation is less clear in the cytoplasm where a decomposition using either the two component model or the bound EB model alone led to the same percentage error. In the latter case, EB must be considered as totally involved in macromolecular interactions.

The decomposition can be applied to the set of records collected in a spectral line image through the cell, such as that reported in Fig. 5b. When applying it, one can isolate

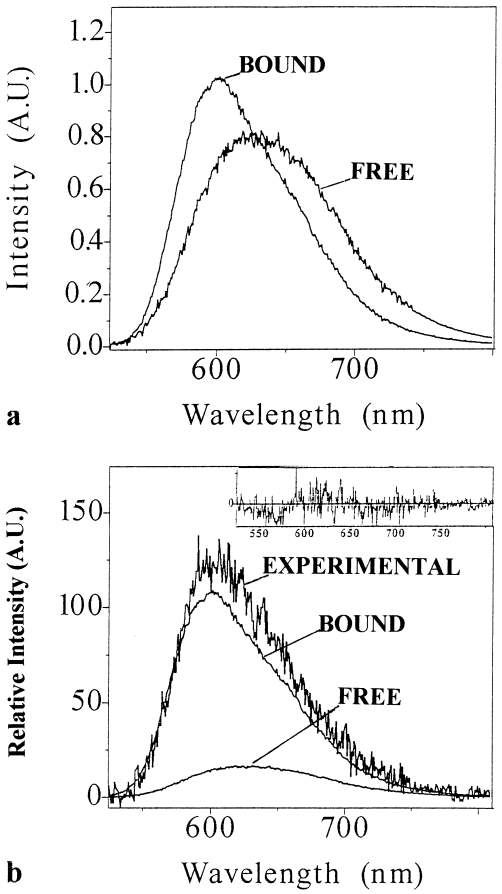

Fig. 6 **a** Reference spectra used for spectral decomposition: free EB (10^{-6} M in PBS) and bound EB (10^{-6} M in PBS with linear pBR 322 DNA, 1 ethidium per 400 bp). Spectra have been normalized on the area. **b** Typical decomposition of a spectrum recorded in the nucleus. In the upper right corner is represented the difference between the observed and the calculated spectra

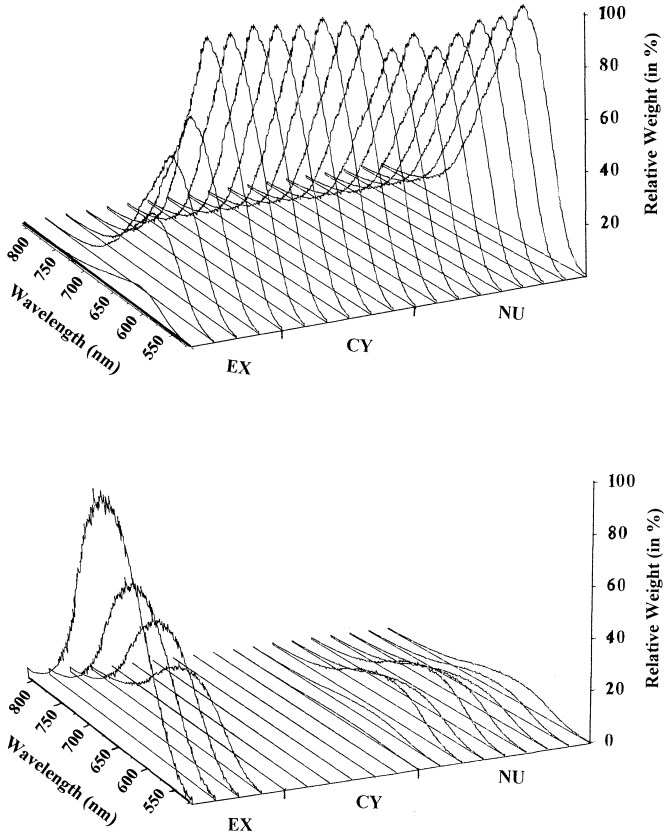

Fig. 7 Decomposition of the spectral line imaging represented in Fig. 5b. In the upper left is shown the relative weight (in percentage) of the bound ethidium in the total intensity of each experimental spectrum. The lower part shows the relative weight (in percentage) of the free ethidium in the total intensity of each experimental spectrum. Direction is as described in Fig. 5b. The sum of the two components gives the 100%

Table 2 Decomposition of the spectral data using a two component model (free and bound EB). The first two columns indicate the percentage of weight in intensity of each component in the three major sites: cytoplasm, nucleus, external medium. The last two columns indicate the percentage of error on the fit when using two components (column 3) or when using only one (bound ethidium, column 4). The values given are means ± standard deviation

	Percentage of bound EB	Percentage of free EB	Percentage of error when using the two component model	Percentage of error when using only the bound EB model
EX	81.5±10	18.5±10	7.7	10
CY	96.5±2.5	3.5±2.5	4.4	4.5
NU	91±3	9±3	5.9	6.8

the relative percentage of each component throughout the cell. Such a decomposition is given in Fig. 7 where the upper part concerns the behaviour of bound EB whereas the lower part concerns that of free EB. The behaviour of free EB is particularly interesting. In the external medium, its relative weight decreases rapidly when approaching the plasma membrane, then vanishes to zero within the cytoplasm and further reaches a relative value up to 16% of the total intensity in certain areas of the nucleus (lower part of the figure). Consistent with these observations, the relative percentage of bound EB increases outside the cells when approaching the plasma membrane; it is then stabilized to nearly 100% within the cytoplasm and diminishes in the nucleus with fluctuations depending on the localization of the laser spot in this compartment.

Discussion

The present study has provided information on ethidium fluorescence in viable salivary gland cells, regarding the spectral characteristics and the intensity of the light emitted in various cellular compartments as a function of time. The fluorescence intensity by itself could not be directly related to the local EB concentration, owing to likely variation of the quantum yield within cellular compartments. This problem remains even after spectra had been decon-

volved to show the relative amounts of free/bound ethidium in various cell domains.

Kinetics of EB intake in viable cells

The kinetics of fluorescence increase due to EB uptake will be discussed mainly in the cytoplasm, where no trace of free ethidium could be detected and where the dye must be considered as most probably engaged in macromolecular interactions. The data could all seemingly be derived from the same EB uptake model by adjusting the temporal factors, although the sorting of salivary gland cells into three groups was convenient for comparison with other living preparations. In chinese hamster ovary cells in culture (Sixou and Teissié 1993), at hourly time resolution and in 2.5×10^{-5} M EB, the time-course of the fluorescence intensity in the cytoplasm, nucleus and nucleolus fitted a classical diffusion model; the half-times of intake and release by intact cells were close to 40 min (after two hours staining). In trypanosomes, the percentage of fluorescent kinetoplasts and nuclei was evaluated at exposure times of 0.5, 1, 6, and 24 hours to EB concentrations ranging from 2.5×10^{-6} M to 1.25×10^{-4} M (Riou 1968). Both organelles present a DNA-rich compartment delimited by a membrane. In the same cells, the kinetoplasts were ten times more intense than the nuclei; this was ascribed to the greater membrane permeability in the former organelles, and to a lack of histone-like proteins able to condense DNA. In comparable ranges of time and EB concentration, a striking similarity can be noted between the evolution of fluorescence intensity in the LN gland cells and that of the occurrence of fluorescent organelles in trypanosomes. This is true when matching Group I to the trypanosome nuclei at 2.5×10^{-6} M EB, or Groups II and III to the kinetoplasts at 2.5×10^{-6} M and 1.25×10^{-5} M EB, respectively. This can be regarded as an indication that, in both studies, the combination of membrane permeability and EB availability can account for a wide range of kinetics.

The volume of the gland was negligible as compared to that of the external medium, and ethidium was still detected externally to the glands at the end of the experiment. It had access to the external (basal) pole of the glandular cells, although the proximity of the coverslip or chamber walls, imposed by the field depth of the microscope objective, could have delayed the diffusion into some cells by several minutes, as has been noted when staining non-viable control preparations with Trypan blue. This quantitative bias is inherent to the present conditions of the kinetic study, and line imaging represents an interesting compromise to reduce data scattering and to disclose meaningful ensemble properties.

Besides physiological differences between the glands themselves, especially with regard to the secretory status (Zhimulev and Kolesnikov 1975), the fluorescence kinetics characterizing the different groups of cells could be modulated by variations of the plasma membrane permeability. Although at 30 min the peripheral cell fluorescence had reached the same level in Groups II and III, and in HN cells, as in osmotically shocked cells, the viability criteria were no longer fulfilled in any of the shocked preparations, while they were still satisfactory, whenever they have been checked, in all the other groups. Thus single criteria are insufficiently refined to define the functional state of living preparations.

Use of two components for spectral deconvolution

The choice of the decomposition of the spectra with the two component model is related to the hydrophilic versus hydrophobic spectroscopic behaviour of the dye. This behaviour has been attributed to proton transfer of the solvent to the EB excited state (Olmsted and Kearns 1977) leading to a decrease in the quantum yield and to a characteristic shift of the spectrum of the dye in water (Free EB). When this proton transfer cannot occur (hydrophobic environment), the quantum yield increases (up to twenty-fold), the fluorescence spectrum is narrowed and the maximum of emission is blue-shifted to 600 nm (Bound EB).

The model spectrum for bound EB was recorded with a very low EB to nucleotide ratio (1:400, mol:mol) to ensure total intercalation of the EB (Waring 1965). Previous work on the interaction of EB with a variety of synthetic polynucleotide sequences shows that the spectral properties of bound EB are independent of the nature of the polynucleotide used, although binding affinities can vary by several orders of magnitude (Bresloff and Crothers 1981). The absorption maximum of bound EB was found at 520 ± 2 nm for polynucleotides and calf thymus DNA, compared to 480 nm for EB in water. The intercalation of EB in a triple-stranded oligonucleotide leads to an enhancement of the fluorescent intensity (Mergny et al. 1991) and fluorescence decay measurements show little variation in the fluorescence lifetime of EB interacting with either Z-DNA or B-DNA (Genest and Malfoy 1986). The behaviour was similar in the case of lipophilic environments such as the plasma membrane (Gitler et al. 1969). As suggested by the spectra recorded in the external medium very near to the gland, and in agreement with our own data of EB in complex protein mixtures, the fluorescent spectral characteristics of EB interacting with proteins lead to λ_{max} and fwhm values close to those observed with EB intercalated in DNA (see below). We note, however, that a detailed spectroscopic study of EB interacting with proteins does not exist at the present time.

The use of EB intercalated between base pairs of linear pBR 322 and of EB in aqueous solution therefore appeared to us as the simplest approach to the spectral decomposition problem.

Ethidium bromide in the extracellular medium

The fluorescence intensity in the extracellular medium was in most cases higher than expected for free ethidium bromide. This is in agreement with spectral characteristics. For measurements made relatively close to the cell, either

by point or line imaging, the λ_{max} mean value was recorded at 602 nm, corresponding to a significant percentage of bound EB (up to 80%). In the spectral line imaging, the further from the plasma membrane the higher was the percentage of free EB. Choosing a definite model to analyze the fluorescence spectrum of interacting EB in the near extracellular medium is not easy. The protein and glycoprotein extrusions from the glands (Beckendorf and Kafatos 1976) seem the most plausible external acceptors of the fluorophore since they can amount to 30% of the total protein content of the gland in the Oregon-R strain presently used (Zhimulev and Kolesnikov 1975). In this case it appears that the fluorescence spectra of EB interacting with a complex mixture of proteins or intercalated in DNA are similar.

Ethidium bromide interactions in the cytoplasm

In the kinetics experiment, one cell was studied in each gland and one microvolume was excited in each cell compartment. In serial records of spectra along the sagittal axis of cells, a fairly regular decrease was observed in the maximal fluorescence intensity when progressing from the basal plasma membrane to the inside of the cell, normally to the membrane. The basal membrane is known to be highly resistant to the outward diffusion of injected ions and fluorescein, while lateral diffusion from cell to cell is free (Loewenstein and Kanno 1964). The cytoplasm could therefore be regarded as a homogeneous fluorescent medium, at the spatial resolution of the observation ($1\times1\times6$ μm in the x, y and z directions) even when sampling each 5 or 2 μm in the xy plane in a time-lapse of several minutes. At this resolution, the so-called membrane sites were in fact composite, including external and intracellular media, which led us not to take them into account for spectral analysis. In all the cells, the spectra from the cytoplasmic sites displayed the same characteristics, with λ_{max} equal to 600 nm. This value was slightly, but consistently, smaller than that measured in the nuclear sites, in agreement with the fact that no free ethidium could be evidenced in the cytoplasm, when applying the two component model deconvolution. Supposedly in vitro, the shift in λ_{max} might indicate either that the medium polarity at the cytoplasmic recording sites was slightly lower than that in the nuclear sites (Radda 1975), or that relatively more ethidium was involved in interactions with substrates in the cytoplasm than elsewhere (Garland et al. 1980). In vivo, their is little probability that a single factor could account for the difference.

Fluorescence emission can be modulated locally by the temperature, the viscosity, the ionic strength, and pH of the medium (Radda 1975; Azzi 1975). Viscosity has been reported to be low and seemingly constant throughout the cytoplasm (Giuliano and Taylor 1995). The intracellular pH has been measured on the same material through selective electrodes about one μm wide at the tip (Wünsch et al. 1993); the pH was 7.48 ± 0.05 in control conditions and increased to 7.72 ± 0.04 on ecdysone activation. Concerning possible temperature effects, it is unlikely that brief (1 s) and weak (20 μW) laser illuminations at five minutes intervals would affect the temperature. Moreover EB is insensitive to temperature changes in the physiological range between 20 and 30 °C (Cuniberti and Guenza 1990); in the control cytogenetic preparations, the genome stained with orcein did not display the puffs characteristic of heat shocked cells.

For these reasons, it seems that the EB spectral characteristics established inside the cytoplasm do not reflect modifications of the physico-chemical environment of the free dye but more likely molecular interactions with different targets. Mitochondrial DNA has been described to be the main target for ethidium bromide inside the cytoplasm (also see Hayashi et al. 1994; Herzberg et al. 1993), but other molecules such as RNAs, proteins, or even intracytoplasmic membrane systems (Golgi, endoplasmic reticulum) cannot be discarded.

Fluorescence emission from the nucleus: free and bound Ethidium

The nuclear membrane does not seem to constitute a barrier to the free diffusion of ethidium (Sixou and Teissié 1993). Accordingly, the paired fluorescence intensity values in the cytoplasm and the nucleus were significantly correlated to each other either at 5 min ($r_s = 0.819$; $p < 0.001$) or at 30 min ($r_s = 0.881$; $p < 0.001$). The ratio of nuclear to cytoplasmic total fluorescence intensities (Table 3) showed that, in most preparations, fluorescence increased faster in the nucleus than elsewhere.

This specificity can be interpreted in several ways. One of them involves nucleolar fluorescence. In several living cells, EB fluorescence has been observed to be much brighter in the nucleolus than in the surrounding nucleus (Sixou and Teissié 1993; Burns 1972; Chadeuf et al. 1995). This was not, however, the case in our material (Fig. 1b). Moreover, the position of the nuclear recording sites was checked during the experiment and was clearly outside the nucleolus. More probably, the nature and/or the availability of EB substrates may change in the nucleus during the experiment. From in vitro studies, the chromosomal puffs ought to emit a brighter fluorescence than does inactive chromatin. Puffs can be observed in quiescent glands (Ashburner 1972; Sass 1995), and have been actually observed

Table 3 Distribution of nuclear vs cytoplasmic fluorescence intensities as a function of time (t) in the three groups of LN cells (G I, II and III) and in HN cells

t (min)	5	10	15	20	25	30
Group						
G I	0.6	0.6	0.7	0.9	0.9	0.7
G II	0.3	0.4	0.5	0.6	0.6	0.7
G III	0.3	0.2	0.2	0.3	0.3	0.6
HN	1	0.9	0.9	1.1	1.4	1.8

in orcein preparation of the EB treated glands (data not shown). Spots with brighter fluorescence have also been detected in line records through several nuclei. Considering the nucleus at the scale of genomial units, one may expect local irregularities in the fluorescence emission, due to the particular organization of chromatin in the present biological material.

The data from spectral analysis support the view that the EB substrates are not quite the same in the nucleus as in the cytoplasm. Firstly, the values of λ_{max} are slightly but consistently higher in the nucleus. Secondly, whereas free ethidium could not be clearly detected within the cytoplasm using the two component (bound and free) model decomposition of the signal, such was not the case in the nucleus (Table 2). The relative apparent concentrations of free to bound ethidium can be tentatively calculated, relying on our own measurements and on the values of fluorescence parameters given in the literature for calf thymus DNA in solution. According to Waring (1965), the ratio of extinction coefficients at 514 nm for bound/free EB is approximately 1.25. Values for the ratio of bound to free quantum yields lie between 21 (Le Pecq and Paoletti 1967) and 11 (Cuniberti et al. 1990). Using the above values, the resulting concentration of free ethidium present in the nucleus can apparently reach 60% to 75% of the total ethidium concentration. These values have to be considered as approximate indices since they rely on extinction coefficient and fluorescence quantum yield variations determined in model systems in vitro. Nevertheless, this amount can be assigned to non intercalated EB inside native chromatin. Preliminary experiments show that it is possible to measure fluorescence lifetimes in living cells. This is expected to yield further quantitative and qualitative information on the interaction of EB with cellular ligands, since this parameter is very sensitive to the type of interaction of EB with macromolecules (Genest and Malfoy 1986; Heller and Greenstock 1994). In any case, the present study of the intracellular distribution of free and interacting ethidium poses questions about the mechanism by which EB and similar intercalating agents are absorbed, carried, exchanged and delivered throughout the cells.

Conclusion

The V45 microspectrofluorometer has been designed with a view to the stereotaxic investigation of the fluorescence emission of living cells. As far as we know, this spectral study is the first one of its kind carried out on a living model relevant in several respects. Firstly, as a whole organ, the salivary gland is closer to actual living tissues than cultured cells can be. Secondly, such a prismatic polarized epithelium is an appropriate model for the study of linear diffusion inside cells. Thirdly, polytene chromosomes present features of the individual mitotic chromosomes together with segments of active chromatin. The apparatus itself, with its limitations and advantages, offers spectral imaging facilities to study the intake of fluorescent probes and to explore the intracellular distribution. Despite the intrinsic limitations presented by EB, this dye constitutes a good probe for the functional state of plasma membranes and the present study sheds a new light on the status of EB as an indicator of irreversibly damaged cell membranes. Another noticeable feature is the finding of a significant amount of free EB in the nucleus, showing the limitation of applying in vitro models to more complex viable living systems. Fluorescent probes specific to defined genomic sequences are now being developed, and the present approach indicates the potential for these further fluorescent spectral studies on living material.

Acknowledgements The authors are specially pleased to acknowledge the obliging and skilful collaboration of Dr. F. Lemeunier (C.N.R.S., Gif s/Yvette) in the cytogenetic part of the present work and the generous gift of Gurr's natural orcein. They are indebted to Dr G. Richards (I.G.B.M.C., Strasbourg) for kind and fruitful suggestions. They are grateful to Drs J.P. Grivet and J.A. Reynaud (C.N.R.S., Orléans) for friendly discussions, and to Marcelle Martineau for willingly nursing the biological material. This work was supported by the C.N.R.S., the Région Centre and the Ministère de l'Enseignement Supérieur et de la Recherche.

References

Angerer LM, Moudrianakis EN (1972) Interaction of ethidium bromide with whole and selectively deproteinized deoxynucleoproteins from calf thymus. J Mol Biol 63:505–521

Ashburner M (1972) Patterns of puffing activity in the salivary gland chromosomes of *Drosophila*. VI Induction by ecdysone in salivary glands of D. melanogaster cultured in vitro. Chromosoma 38:255–281

Ashburner M (1990) Puffs, genes, and hormones revisited. Cell 61:1–13

Azzi A (1975) The application of fluorescent probes in membrane studies. Quart Rev Biophys 8:237–316

Beckendorf SK, Kafatos FC (1976) Differenciation in the salivary glands of *Drosophila* melanogaster: characterization of the glue proteins and their developmental appearance. Cell 9:365–373

Benyajati C, Worcel A (1976) Isolation, characterization and structure of the folded interphase genome of *Drosophila melanogaster*. Cell 9:393–407

Bresloff JL, Crothers DM (1981) Equilibrium studies of ethidium-polynucleotide interactions. Biochemistry 20:3547–3553

Bicknell GR, Cohen GM (1995) Cleavage of DNA to large kilobase pair fragments occurs in some forms of necrosis as well as apoptosis. Biochem Biophys Res Com 207:40–47

Brodie S, Giron J, Latt SA (1975) Estimation of accessibility of DNA in chromatin from fluorescence measurements of electronic excitation energy transfer. Nature 253:470–471

Burns VWF (1972) Location and molecular characteristics of fluorescent complexes of ethidium bromide in the cell. Exp Cell Res 75:200–206

Chadeuf G, Egret-Charlier M, Villa AM, Favard C, Doglia SM, Vigny P (1995) In situ spatial distribution and spectroscopic properties of Ethidium Bromide inside living cells. J Trace Microprobe Tech 13:255–257

Cook PR, Brazell IA (1978) Spectrofluorometric measurement of the binding of ethidium to superhelical DNA from cell nuclei. Eur J Biochem 84:465–477

Cuniberti C, Guenza M (1990) Environment-induced changes in DNA conformation as probed by ethidium bromide fluorescence. Biophys Chem 38:11–22

Darzynkiewicz Z, Traganos F, Kapuscinski J, Staiano-Coico L, Melamed MR (1984) Accessibility of DNA in situ to various fluo-

rochromes: relationship to chromatin changes during erythroid differentiation of Friend leukemia cells. Cytometry 5:355–363
Dey CS, Majumder GC (1988) A simple quantitative method of estimation of cell-intactness based on ethidium bromide fluorescence. Biochem Internat 17:367–374
Dutch Boltz RC, Fischer PA, Wicker LS, Peterson LB (1994) Single UV excitation of Hoechst 33342 and ethidium bromide for simultaneous cell cycle analysis and viability determinations on in vitro cultures of murine B lymphocytes. Cytometry 15:28–34
Ericsson C, Grossbach U, Björkroth B, Daneholt B (1990) Presence of histone H1 on an active Balbiani ring gene. Cell 60:73–83
Garland F, Graves DE, Yielding LW, Cheung HC (1980) Comparative studies of the binding of ethidium bromide and its photoreactive analogues to nucleic acids by fluorescence and rapid kinetics. Biochemistry 19:3221–3226
Genest D, Malfoy B (1986) Fluorescence decay of ethidium bromide in the presence of the Z-conformation of poly (dG-dC) and of poly (dG-dC) modified by chlorodiethylenetriamine platinium (II) chloride. Biopolymers 25:507–518
Gitler C, Rubalcava B, Caswell A (1969) Fluorescence changes of ethidium bromide on binding to erythrocyte and mitochondrial membrane. Biochem Biophys Acta 193:475–478
Giuliano KA, Taylor L (1995) Measurement and manipulation of cytoskeletal dynamics in living cells. Curr Biol 7:4–12
Gruzdev AD, Shurdov MA (1992) Topological state of DNA in polytene chromosomes. Biochem Biophys Acta 1131:35–40
Hartwig M (1979) Molecular mechanisms in cancerogenesis: chromosomal DNA unwinding modelled by ethidium bromide. Stud Biophys 75:71–77
Hayashi JI, Takemitsu M, Goto Y, Nonaka I (1994) Human mitochondria and mitochondrial genome function as a single dynamic cellular unit. J Cell Biol 125:43–50
Heinen E, Lepoint A, Bassler R, Goessens G (1974) Effects of ethidium bromide on chick fibroblasts and mouse Ehrlich tumor cells cultivated in vitro. Cytological and cytochemical observations. Beitr Path Bd 153:363–369
Heller DP, Greenstock CL (1994) Fluorescence lifetime analysis of DNA intercalated ethidium bromide and quenching by free dye. Biophys Chem 50:305–312
Herzberg NH, Middelkoop E, Adorf M, Dekker HL, Van Galen MJ, Van den Berg M, Bolhuis PA, Van den Bogert C (1993) Mitochondria in cultured human muscle cells depleted of mitochondrial DNA. Eur J Cell Biol 61:400–408
Himpens B, De Smedt H, Droogmans G, Casteels R (1992) Differences in regulation between nuclear and cytoplasmic Ca^{2+} in cultured smooth muscle cells. Am J Physiol C95–C105
Huet F, Ruiz C, Richards G (1993) Puffs and PCR: the in vivo dynamics of early gene expression during ecdysone responses in *Drosophila*. Development 118:613–627
Kattstrom PO, Nilsson BO (1992) Preparation of human chromosomes for high resolution scanning electron microscopy. Arch Histol Cytol 55 Suppl:53–56
Kuwano A, Kajii T (1991) High-resolution banding in chromosomes of B lymphoblastoid cells and cultured skin fibroblasts. Cytogenet Cell Genet 56:212–213
Latt SA, Langlois RG (1990) Fluorescent probes of DNA microstructure and DNA synthesis. In: Myron RM, Lindmo T, Mendelsohn ML (eds) Flow cytometry and sorting, ch 14. Wiley-Liss Inc, New York, pp 249–290
Le Pecq JB (1972) Use of ethidium bromide for separation and determination of nucleic acids of various conformational forms and measurement of their associated enzymes. Meth Biochem Anal 20:41–86
Le Pecq JB, Paoletti C (1967) A fluorescent complex between Ethidium Bromide and nucleic acids. Physical-chemical characterization. J Mol Biol 27:87–106
Levi-Setti R, Chabala JM, Smolik S (1994) Nucleotide and protein distribution in BrdU-labelled polytene chromosomes revealed by ion probe mass spectrometry. J Microscopy 175 pt1:44–53
Loewenstein WR, Kanno Y (1964) Studies on an epithelial (gland) cell junction. I. Modifications of surface membrane permeability. J Cell Biol 22:565–586
Mattern MR, Painter RB (1979) Dependence of mammalian DNA replication on DNA supercoiling. I. Effects of ethidium bromide on DNA synthesis in permeable chinese Hamster ovary cells. Biochem Biophys Acta 563:293–305
Mergny JL, Collier D, Rougée M, Montenay-Garestier T, Helene C (1991) Intercalation of ethidium bromide into a triple-stranded oligonucleotide. Nucleic Acids Res 19:1521–1526
Olmsted (III) J, Kearns DR (1977) Mechanism of ethidium fluoroescence enhancement on binding to nucleic acids. Biochemistry 16:3647–3654
Pager J, Favard C, Locker D, Vigny P (1995) In vivo studies of chromatin: preliminary investigations on salivary glands of *Drosophila* using fluorescence microscopy. J Trace Microprobe Tech 13:259–261
Paoletti J (1979) Relaxation of chromatin structure induced by ethidium binding. Involvement of the intercalation process. Eur J Biochem 100:531–539
Paoletti J, Magee BB, Magee PT (1977) The structure of chromatin: interaction of ethidium bromide with native and denatured chromatin. Biochemistry 16:351–357
Prokuryakov SY, Gabai VL, Mosin AF, Ryabchenko NI (1989) DNA degradation, and changes in permeability and morphology of cells of the Ehrlich ascite tumor under aerobic incubation without glucose. Tsitologiya 31:690–695
Radda GK (1975) Fluorescent probes in membrane studies. In: Korn ED (ed) Methods in membrane biology, no 4, ch 3. Academic Press, San Diego, pp 97–188
Riou G (1968) Disparition de l'ADN du kinétoplaste de *Trypanosoma Cruzi* cultivé en présence de bromure d'ethidium. C R Acad Sci Paris 266:250–252
Rykowski MC, Parmelee SJ, Agard DA, Sedat JW (1988) Precise determination of the molecular limits of a polytene chromosome band: regulatory sequences for the *Notch* gene are in the interband. Cell 54:461–472
Saitoh Y, Laemmli UK (1994) Metaphase chromosome structure: bands arise from a differential folding path of the highly AT-rich scaffold. Cell 76:609–622
Santi P, Papa S, Del Coco R, Falcieri E, Zini N, Marinelli F, Maraldi NM (1987) Modifications of the chromatin arrangement induced by ethidium bromide in isolated nuclei, analyzed by electron microscopy and flow cytometry. Biol Cell 59: 43–54
Santisteban MS, Montmasson MP, Giroud F, Ronot X, Brugal G (1992) Fluorescence image cytometry of nuclear DNA content versus chromatin pattern: a comparative study of ten fluorochromes. J Histochem Cytochem 40:1789–1797
Sass H (1995) Transcription of heat shock gene loci versus non-heat shock loci in *Chironomus* polytene chromosomes: evidence for heat-induced formation of novel putative ribonucleoprotein particles (hsRNPs) in the major heat shock puffs. Chromosoma 103:528–538
Sixou S, Teissié J (1993) Exogenous uptake and release of molecules by electroloaded cells: a digitized videomicroscopy study. Bioelectrochem Bioenerg 31:237–257
Slonimski PP, Perrodin G, Croft JH (1968) Ethidium bromide induced mutations of yeast mitochondria: complete transformation of cells into respiratory deficient non-chromosomal "petites". Biochem Biophys Res Comm 30:232–239
Sumner AT (1992) Inhibitors of topoisomerases do not block the passage of human lymphocyte chromosomes through mitosis. J Cell Sci 103:105–115
Sumner AT (1994) Functional aspects of the longitudinal differentiation of chromosomes. Eur J Histochem 38:91–109
Tekle E, Astumian RD, Chock PB (1991) Electroporation by using bipolar oscillating electric field: an improved method for DNA transfection of NIH 3T3 cells. Proc Natl Acad Sci USA 88:4230–4234
Thresher RJ, Griffith JD (1990) Intercalators promote the binding of RecA protein to double-stranded DNA. Proc Natl Acad Sci USA 87:5056–5060
Valisa P, Favard C, Roussel B, Ballini JP, Amirand C, Sharonov S, Chadeuf G, Egret-Charlier M, Manfait M, Da Silva E, Vigny P

(1995) Characteristics of a new UV-visible microspectrofluorometer devoted to subcellular studies. J Trace Microprobe Tech 13:251–253

Vergani L, Gavazzo P, Mascetti G, Nicolini C (1994) Ethidium bromide intercalation and chromatin structure: a spectropolarimetric analysis. Biochemistry 33:6578–6585

Waring MJ (1965) Complex formation between Ethidium Bromide and nucleic acids. J Mol Biol 13:269–282

Weston KM, Alsalami M, Raison RL (1994) Cell membrane changes induced by the cytolytic peptide, melittin, are detectable by 90° laser scatter. Cytometry 15:141–147

Woodward CT, Baehrecke EH, Thummel CS (1994) A molecular mechanism for the stage specificity of the *Drosophila* prepupal genetic response to ecdysone. Cell 79:607–615

Wünsch S, Schneider S, Schwab A, Oberleithner H (1993) 20-OH-ecdysone swells nuclear volume by alkalinization in salivary glands of *Drosophila melanogaster*. Cell Tissue Res 274: 145–151

Zhimulev IF, Kolesnikov NN (1975) Synthesis and secretion of mucoprotein glue in the salivary gland of *Drosophila melanogaster*. Wilhelm-Roux's Arch 178:15–28